UCRL - 77311
PREPRINT
Conf-750975--4

LAWRENCE LIVERMORE LABORATORY
University of California/Livermore, California

Collisional Quenching of Metastable X-Ray Emitting States in a Fast Beam of He-Like Fluorine

D. L. Matthews
R. J. Fortner

September 1975

This paper was prepared for submission to
4th International Conference
Beam-Foil Spectroscopy and Heavy Ion Atomic Physics
Gatlinburg, TN, September 15-19, 1975

COLLISIONAL QUENCHING OF METASTABLE X-RAY EMITTING STATES IN A FAST BEAM OF He-LIKE FLUORINE*

D. L. Matthews and R. J. Fortner

Lawrence Livermore Laboratory

Livermore CA 94550

ABSTRACT

High resolution x-ray spectral measurements are used to determine the relative intensity of He-like fluorine x-ray transitions, $2\ ^3P_1 \rightarrow 1\ ^1S_0$ and $2\ ^1P_1 \rightarrow 1\ ^1S_0$, produced fluorine collisions with Ne, Ar, and Kr gas targets at various pressures and in thin carbon foils and a thick carbon slab. The relative intensities are observed to be strong functions of both target density and incident charge Z. These effects are attributed to strong collisional quenching of both initial states by subsequent large impact parameter collisions. The data permit extraction for the first time of the total quenching cross sections (σ_Q) for fast fluorine ions in both states. A strong enhancement of the relative intensity of the $2\ ^3P_1$ is observed for F^{7+} projectiles. This strong enhancement is attributed to selective excitation of metastable states in the beam, i.e. $1s2s\ ^3S_1$, into the $1s2p\ ^3P_1$ state. Finally, the data for foil and solid targets are used to obtain new information on the excitation states of ions moving in solids. High resolution measurements of the radiative electron capture (REC) peak are reported and analyzed for the first time.

*Work performed under the auspices of the U. S. Energy Research and Development Administration, under contract No. W-7405-Eng-48

The study of collisional quenching of atomic states in ion-atom collisions has received considerable attention. However, the extension of this type study to metastable x-ray emitting states in high velocity helium-like ions (i.e. Z > 2) has received little or no attention. In the following we will show that the cross section for collisional quenching of metastable x-ray emitting states for high velocity ion-atom collisions is appreciable. In fact, we demonstrate that the effects of collisional quenching can dominate the spectral intensities of x-ray lines formed under single inner shell collision conditions. First, measurements of gas target spectra will be reported for different gas pressures and the collisional quenching cross section, σ_Q, will be determined for the $1s2p\ ^3P_1$ state in fluorine. Then the data for thin carbon foils will be used to determine σ_Q for the $1s2p\ ^1P_1$ state in fluorine. New information on the "dynamic fluorescence yield" for individual x-ray transitions are obtained for ions moving in solids. Finally, high resolution measurements of the radiative electron capture (REC) x-rays of conduction electrons are also obtained and analyzed.

Fig. 1 demonstrates the principal effects observed in this measurement. The transitions $1s2p\ (2\ ^3P_1) \rightarrow 1s^2\ (1\ ^1S_0)$ and

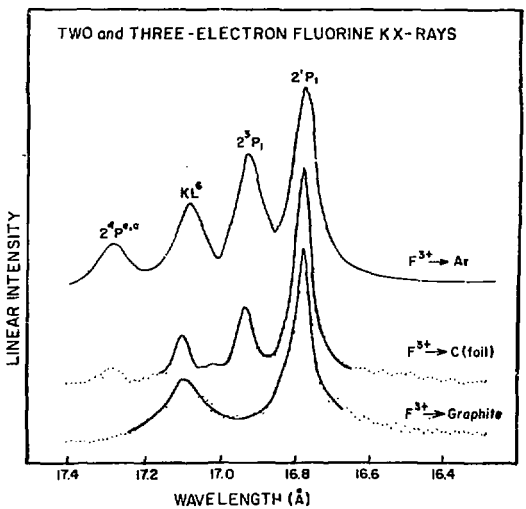

Fig. 1

$1s2p\ (2\ ^1P_1) \rightarrow 1s^2\ (1\ ^1S_0)$ from the decay of two electron fluorine ions excited in gas, foil and solid targets are shown. The $^3P_1/^1P_1$ variation with target gas density in F^{5+} + Ne, Ar, and Kr collisions is shown in Fig. 2. In going from 10 to 200 microns, a monotonic decrease in the ratio is observed. To explain this variation, a theoretical formulation for the intensity of a given atomic state in a fast moving ion beam is required.

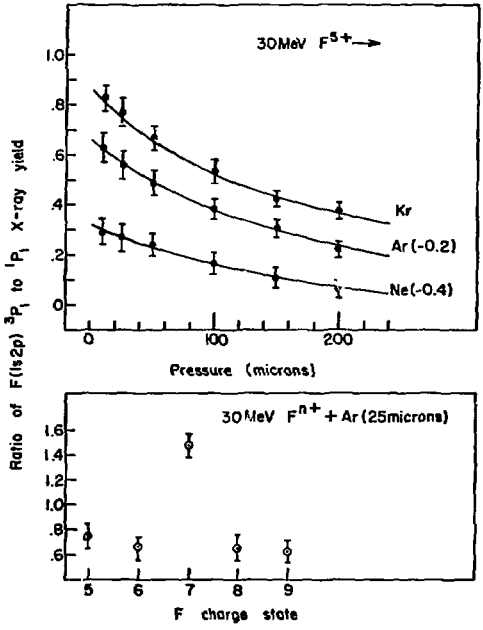

Fig. 2

The number density $n(cm^{-3})$ of fast excited ions in state j at a given distance x from the entrance to the target satisfies the differential equation

$$\frac{dn_j}{dx} = \frac{-n_j}{v\tau} - n_j N\sigma_Q + \frac{\sigma_0 N(I-n_j v)}{v} \qquad (1)$$

where v is the ion velocity, I is the beam flux (cm^{-2}-sec^{-1}), σ_0 is the cross section for producing j, N is the target gas density, τ is the atomic lifetime of state j and σ_Q is the total effective cross section for collisional quenching or extinction of excited state j. This σ_Q may be the result of several loss terms due to collisional excitation/de-excitation out of state j. If at x = 0, $n_j = 0$, then Eq. 1 has the solution

$$n_j = \frac{\sigma_0 IN}{v\beta}\left[1 - e^{-\beta x}\right] \qquad (2)$$

where $\beta = [N(\sigma_0 + \sigma_Q) + 1/v\tau]$. Consider for an example a 30 MeV fluorine beam and the $1s2s\ ^3P_1$ state ($\tau = 0.54 \times 10^{-9}$ s). In a solid $1/\beta \sim 10$ Å and in a gas $1/\beta < 1.1$ cm. In both cases equilibrium is easily obtainable, thus

$$n_j = \frac{\sigma_0 IN}{v\beta} \qquad (3)$$

In a gas the number of photons emitted is

$$R_j = \int_0^L \frac{\sigma_0 IN}{1 + N\sigma' v\tau}\, dx = \frac{\sigma_0 INL}{1 + N\sigma' v\tau} \qquad (4)$$

For prompt transitions such as from the $1s2p\ 2\ ^1P_1$ state ($\tau = 1.8 \times 10^{-13}$ s) $N\sigma' v\tau << 1$ for meaningful σ' and gas densities of interest. Eq. 4 then becomes simply $R_j(^1P_1) = \sigma_0 INL$. For the $2\ ^3P_1$ state $N\sigma' v\tau$ is not necessarily small compared to 1. Under these circumstances we can get an expression for the relative $2\ ^3P_1$ to $2\ ^1P_1$ x-ray yields which is given by

$$R' = \frac{R_0}{1 + N\sigma' v\tau} \qquad (5)$$

where R_0 is the ratio of x-ray production cross sections for the $^3P_1$ to $^1P_1$ states. The expression for R' represents a simple formula for predicting the reduction in $^3P_1/^1P_1$ relative intensities with increasing gas density, and can be fit to experiment thus determining R_0 and σ'. In the analysis R_0 was determined by extrapolating the data to near zero gas pressure while σ' was determined by the best fits to the data shown in Fig. 2. The fitted R' values are shown in Fig. 2 by the solid line. Over a pressure change of a factor of 20 we get good agreement with experiment. The values we obtain for $\sigma' = \sigma_0 + \sigma_Q$ are much too large in comparison with measured inner shell vacancy production cross sections thus $\sigma' \approx \sigma_Q$. The values obtained for σ_Q and R_0 are shown in Table 1.

TABLE 1

Target	$R_0(\pm 0.10)$	$\sigma_Q(10^{-16}\ cm^2)$	$\sigma(\times 10^{-16}\ cm^2)$
Ne (Z = 10)	0.71	0.7 ± 0.2	0.9
Ar (Z = 18)	0.86	1.5 ± 0.4	2.4
Kr (Z = 36)	0.87	2.0 ± 0.6	3.5

Another interesting aspect of these data is the dependence of the relative intensity of the $^3P_1$ and $^1P_1$ x-ray lines on the incident charge state of the fluorine projectile as can be seen in Fig. 2b. For all charge states except 7^+ the relative yields are constant. For charge state 7^+, the $^3P_1$ line is enhanced by almost a factor of two. For 7^+ projectiles, a predominant mode for production of the $^3P_1$ and $^1P_1$ lines is electron excitation since the number of electrons in initial and final states is the same. In this type of collision the long range coulomb interaction is expected to populate selectively into excited states not requiring a spin change (i.e. spin flip). At first this seems to be contradicted by our data which indicates that the $^3P_1$ state is selectively populated from a ground state $1s^2\ ^1S_0$. However, we attribute the selective enhancement of the $^3P_1$ state to be due to excitation of the metastable 1s2s $^3S_1$ states and not the $1s^2\ ^1S_0$ state. The presence of metastable 1s2s $^3P_1$ states in the incident F^{7+} beam is a result of their long mean free path $v\tau = 2.3 \times 10^5$ cm as compared to 1.4×10^3 cm path length from post stripper foil to target gas cell.

The quenching cross section for the 1s2p $^1P_1$ state can be obtained from the thin foil data. Before starting this discussion, however, some general conclusions obtained from the total x-ray yield from these targets should be discussed. The x-ray spectra were measured for several foil thicknesses ranging from 5 to 200 $\mu g/cm^2$. Except for small differences in going from 5 to 10 $\mu g/cm^2$ in the hydrogen-like lines the x-ray yields and relative intensities were constant--independent of foil thickness. From these results we can conclude that nearly all the x-ray emission observed when viewing beam-foil interactions comes from outside the foil. This general conclusion appears true for all the normal x-ray lines. The REC peak (see below) was observed for only the thickest foils indicating that it is a strong function of foil thickness. It appears that these x-rays come from transitions taking place predominantly in the foil consistent with the κEC mechanism.

Comparisons of the relative intensity of individual x-ray lines in foil and solid targets is instructive. Consider for example the normal 2p → 1s transitions for the helium- and lithium-like lines. These are compared for gas, foil, and thick targets in Fig. 1. In this figure we can have 4 different x-ray transitions in order of increasing energies, the ^4P transitions which includes transitions from the $1s2s2p$ and $1s2p^2$ configurations and J components of 1/2, 3/2, and 5/2 (these states have lifetimes ranging from 1 to 12 ns), the next line comes predominantly from the ^2P states again from the $1s2s2p$ and $1s2p^2$ configurations (these states have lifetimes of approximately 10^{-13} s), the third line is the $^3P_1$ state from the $1s2p$ configuration (0.54 ns lifetime), and the last line is the $^1P_1$ state from the $1s2p$ initial configuration (1.8×10^{-13} s lifetime). In the gas target spectra we see that the two lines in the same series are about equally populated. In the foil produced spectra the relative intensities are quite different. The longer lived components in the spectra appear considerably reduced. For solid spectra the longer lived components are reduced even further in fact within the limits of our detection system they are completely gone.

Inside a solid the probability that a state will decay giving an x-ray is reduced. Consider, for example, the helium-like states, $^3P_1$ and $^1P_1$ which have essentially unit atomic fluorescence yield. Inside the foil the probability that a state will emit an x-ray is given by

$$\frac{1/\tau_R}{1/\tau_R + N\sigma_Q v} \tag{6}$$

where τ_R is the intrinsic radiative lifetime. For the $^3P_1$ state in helium-like fluorine, $N\sigma_Q v \approx 10^{15}$ s^{-1}, thus the probability that this state emits an x-ray in the solid, i.e. dynamic fluorescence yield, is $\approx 10^{-6}$. σ_Q for the $^1P_1$ helium-like state can be estimated from the relative intensities of the $^3P_1$ and $^1P_1$ lines in the foil produced spectra. σ_Q has been measured to be approximately the same for both the $^3P_1$ and $^1P_1$ lines in gas target measurements. Since essentially all the x-rays are emitted outside the foil and both lines have unit fluorescence yields the relative intensities are obtained from Eq. 2 as

$$\frac{Y(^3P_1)}{Y(^1P_1)} = \frac{N\sigma_Q(^1P_1) + N\sigma_Q(^1P_1) + 1/v\tau(^1P_1)}{N\sigma_Q(^3P_1)} \tag{7}$$

Using estimates of σ_Q of 10^{-18} cm^2 and $\sigma_Q(^3P_1)$ of 10^{-16} cm^2 and a measured $Y(^3P_1)/Y(^1P_1)$ of $\sim$0.1 we obtain an estimated $\sigma_Q(^1P_1)$ of 8×10^{-18} cm^2. Thus, the probability that this state

will x-ray decay in the solid is ∿7%. These observations are consistent with the solid target data in Fig. 1. In the solid target spectra the $^3P_1$ state is not observed and the small yield of x-rays obtained from the solid graphite target (the yield of characteristic x-rays from ions impinging on a thick target slab was only 20% of that observed for a 5 μg/cm^2 foil) is then due to the small probability for x-ray decay in the solid.

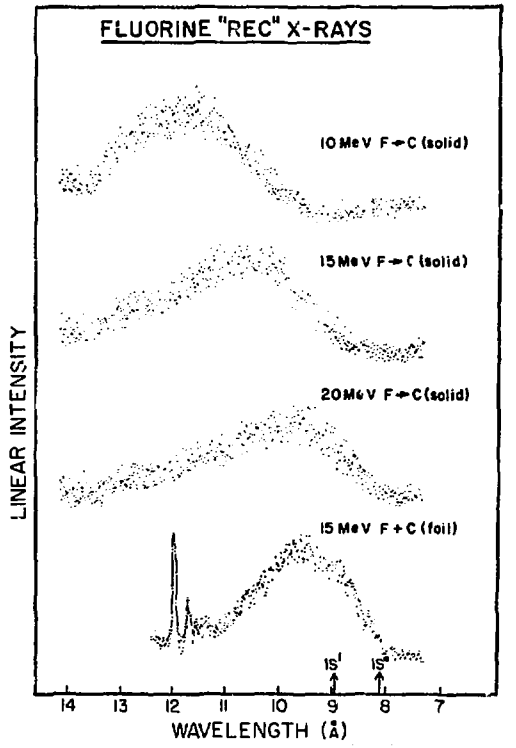

Fig. 3

In Fig. 3 the REC peaks for various energy fluorine ions incident on a solid and 15 MeV ions incident on a 100 μg/cm^2 foil are shown. The existence of the large REC peak indicates that

there are substantial amounts of zero electron and one electron ground state (1s) atoms moving in the solid. For these types of atoms REC is the predominant mechanism for filling of the K vacancies since there are no outer shell electrons present. The centroid energy of the REC peak moves as the incident energy changes. The value of the centroid energy is still slightly lower than one would expect, consistent with other observations and probably due to the electronic screening of the ion due to the presence of electrons in the solid. For the solid the REC peak is skewed to lower energies. This is due to REC in ions which have lost considerable energy in the solid. The measured half width for the REC peak in the 100 $\mu g/cm^2$ foil is 260 eV. The contribution to the width of this line due to energy loss in the foil is negligible (<20 eV). The width of the REC peak assuming a Fermi distribution is $4\sqrt{T_R T_f}$ where T_R is the kinetic energy of the captured electron relative to incident ion and T_f is the width of the conduction band. Our measured width was inconsistent with the assumption of a single REC peak and a reasonable Fermi energy, T_f. The REC line was then analyzed by assuming it was composed of two components of equal width involving capture into both the $1s^0$ and $1s^1$ cores. The energy separation was assumed to be the theoretical value of 120 eV. Assuming Gaussian line shapes this resulted in a REC width of 180 ± 20 eV implying a value of T_f of 4.7 ± 1.1 eV.